An Equation for the Calculation of Saturated Water Contents in Silicate Melts: A New Version

Ya. Yu. Gnuchev[a], *, D. A. Bychkov[a], **, and E. V. Koptev-Dvornikov[a], ***

[a] Faculty of Geology, Lomonosov Moscow State University, Moscow, 119991 Russia
*e-mail: gnuchevyakov@mail.ru
**e-mail: dmibychkov@gmail.com
***e-mail: ekoptevmail@gmail.com

Abstract—A set of experimental data compiled from the literature comprises results of 394 quenching experiments that characterize the saturated water content within wide ranges of intensive parameters of silicate systems. Analysis of the main types of published models of water solubility in silicate melt showed that the equation by G. Moore et al. (1998) best describes experimental results. The Moore equation, converted to an exponential form, was recalibrated on an extended set of experimental data, and the new coefficients for this equation are: $a = 918$; $b\text{Al}_2\text{O}_3 = -0.712$; $b\text{FeO} = -0.749$; $b\text{Na}_2\text{O} = 0.806$; $c = 1.087$; and $d = -11.45$. The Moore equation with new coefficients makes it possible to predict the saturated water content in silicate melts accurate to ± 1 to ± 2 relative % in the range of melt compositions from basalt to rhyolite, pressures from atmospheric to 15 kbar, and temperatures from 550 to 1300°C.

INTRODUCTION

Currently available systems of compositometer equations (i.e., equations for calculating the composition of minerals in equilibrium with melt under specified parameters) involve variables that are experimental data: temperature, pressure, chemical composition of the system, and oxygen fugacity (Ar'yaeva et al., 2016; Koptev-Dvornikov et al., 2012, 2019, 2020; Romanova et al., 2020). However, these compositometers were derived by means of statistical processing results of anhydrous experiments, whereas the great majority of natural magmas and lavas contain variable concentrations of water.

Numerous experiments have been conducted with the involvement of pure H_2O fluids and those of complex composition. In this publication, we constrained ourselves to analysis of interaction between silicate melt and pure H_2O fluid.

The following two problems should be resolved to be able to account for the effect of water on melt differentiation in a chamber. When compiling a representative dataset, we became aware that data of only 20% of the experiments referred to as water-saturated by the authors involve information on water concentrations in the melts, which leads to that much of the data should be rejected from statistical processing. At the same time, water is an incompatible component at the crystallization of rock-forming minerals in mafic systems and, hence, enriches the residual melts. It is necessary to know the highest water concentration in melt above which water makes up an individualized vapor phase.

This problem can be resolved by developing an equation that would enable the calculation of water saturated concentration in melt. Such an equation would make it possible to also resolve the problem of the limited volume of the dataset on hydrous experiments. A.A. Ariskin and G.S. Barmina were the first to use such an equation to calculate water concentrations in hydrous experiments in which water contents had not been unmeasured, and this made it possible to expand the potential size of the dataset for deriving melt—mineral thermobarometers (Ariskin and Barmina, 2000). Moreover, dissolved volatile gases significantly modify the density and viscosity of the magmas and thus play a decisive role in magma ascent. The density and viscosity of ascending magmas can be evaluated based on models for the solubility of volatile components that make it possible to calculate changes in the compositions of the melt and vapor as functions of pressure and temperature (Newman and Lowenstern, 2002). Such models are also useful for planning experiments with hydrous systems and for testing experimental data on water solubility in melts.

Several equations of the type have already been proposed, but they yield different values of water contents
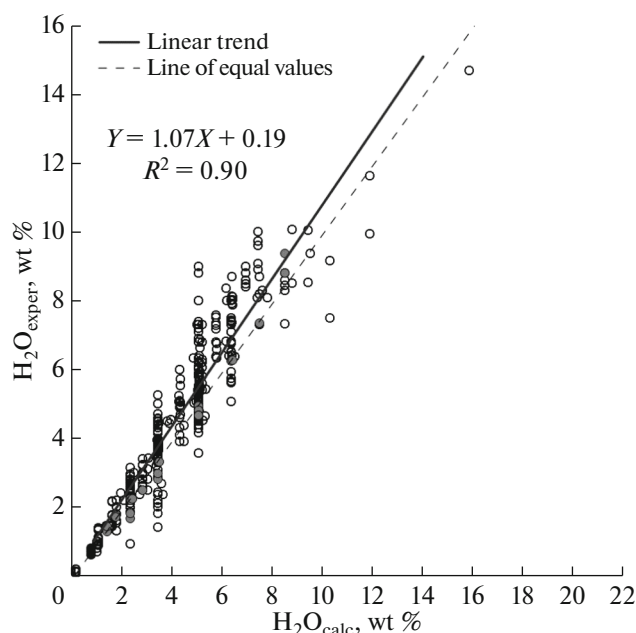
Fig. 1. Comparison of water solubility calculated by the model (Shishkina et al., 2010) with experimental data (data of 412 experiments in the dataset): solid circles are experimental data used by the authors to calibrate the equation, open symbols are other data from our dataset.

at the same parameters. Our study was aimed at deriving an equation that would best fit all currently available experimental data. Such an equation could be obtained by either selecting from all preexisting models for water solubility or by developing an original equation.

COMPILING A SET OF SELECTED DATA OF WATER-SATURATED EXPERIMENTS

Previously, most of the experimentalists derived their equations based on a limited amounts of data on original experiments in hydrous systems and more rarely used data sets compiled from several publications (these datasets comprised results of approximately 20 to 100 experiments with pure H_2O fluid). In analyzing the literature, we have found 33 publications presenting data on dissolved water in hydrous melt according to results of 412 experiments.

A principal data source from which out dataset was compiled was the INFOREX database (Ariskin et al., 1996), and we also compiled experimental data from publications whose data were utilized to derive earlier equations (Shishkina et al., 2010; Berndt et al., 2002; Botcharnikov et al., 2004; Moore at al., 1995, 1998; Carrol and Blank., 1997; Silver et al., 1990; Shaw et al., 1963; Liu et al., 2005; Yamashita, 1999; Schmidt and Behrens, 2008).

The criteria used to include experimental data in the set were the availability of information on equilibrium between melt of known composition and a fluid phase that contained no components other than water.

REVIEW OF PREEXISTING EQUATIONS FOR CALCULATING WATER MOLE FRACTION IN MELT

Several equations have been proposed to describe the saturated solubility of water in silicate melts. When selecting the equations, we proceeded from the simplest (in terms of both their derivation and the calibration, which involve a single variable) to more complicated ones.

The simplest equations that are often applied describe saturated water concentration in silicate melt as a function of pressure alone (Carroll and Blank., 1997; Moore et al., 1995, 1998; Zhang et al., 2007). Of the equations of this type, we selected Eq. (1) in (Shishkina et al., 2010), because this equations has been derived from data of experiments within a broad pressure range.

Equation (Shishkina et al., 2010)

Equation (1) proposed in (Shishkina et al., 2010) is

$$\ln C_{H_2O} = 0.2351 P^{0.5758}, \tag{1}$$

where C_{H_2O} is the saturated H_2O concentration (in wt %) in melt, and P is the pressure in MPa.

The ranges of the intensive parameters in the dataset from which the equation has been derived are a temperature of 1250°C, pressure of 1 bar to 5 kbar, and water concentrations of 1 to 9 wt %; the size of the set is 27 data points, the composition is tholeiitic basalt.

Comparison of calculation results yielded by this model with experimental data from our dataset (Fig. 1) shows that a single calculated concentration corresponds to a wide range of experimentally determined water concentrations, which led us to the conclusion that other intensive parameters have also be taken into account.

Equation (Liu et al., 2005)

Another equation for the pressure dependence of the saturated water concentration was presented in (Liu et al., 2005), and unlike the previous equation, this one involves temperature

$$C_w = \frac{354.94\sqrt{P_w} + 9.623 P_w - 1.5223 P_w^{\frac{3}{2}}}{T} \tag{2}$$

$$+ 0.0012439 P_w^{\frac{3}{2}} + P_{CO_2} \times 10^{-4}(-1.084\sqrt{P_w} - 0.1362 P_w),$$

where C_w is saturated water concentration (in wt %), T is the temperature in K, P_w is the partial H_2O pressure in MPa, and P_{CO_2} is the partial CO_2 pressure in MPa.

The ranges of the intense parameters in the dataset is a temperature of 700−1200°C, pressure of 1 bar to 5 kbar, and saturated water concentration of 0.5 to 11 wt %. The equation was derived by fitting data of
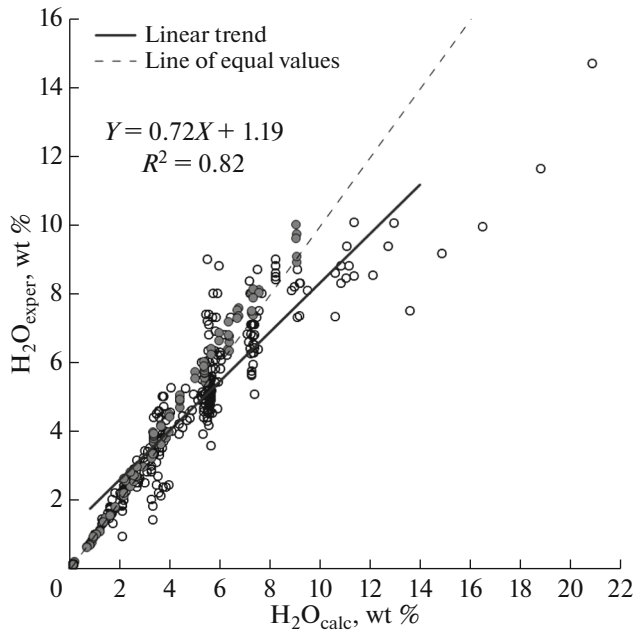
Fig. 2. Comparison of water solubility calculated by the model (Liu et al., 2005) with experimental data (data of 412 experiments in the dataset): solid circles are experimental data used by the authors to calibrate the equation, open symbols are other data from our dataset.
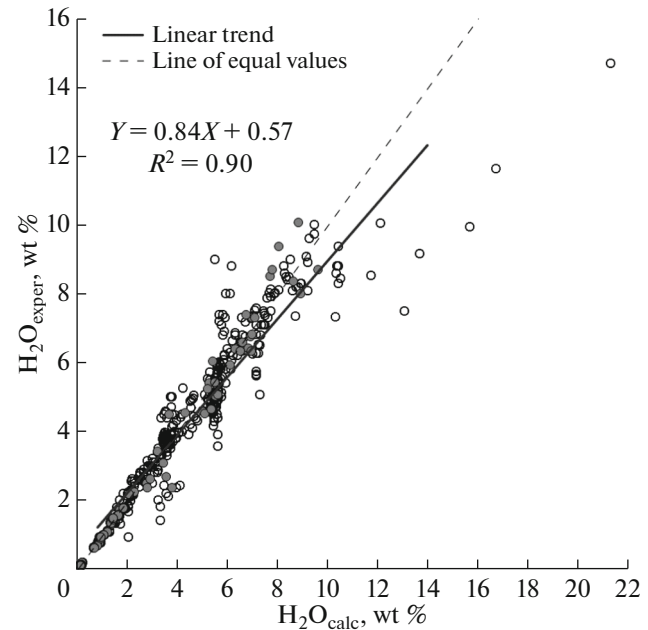
Fig. 3. Comparison of water solubility calculated by the model (Zhang et al., 2007) with experimental data (data of 412 experiments in the dataset): solid circles are experimental data used by the authors to calibrate the equation, open symbols are other data from our dataset.

299 experimental runs, with about 80 of them conducted with natural (mostly felsic) compositions and a pure H_2O fluid phase. These data points are shown in Fig. 2.

Comparison of the calculation results of this model with experimental data from our dataset (Fig. 2) shows that, on the one hand, the experimental data are better fitted at low concentrations, and on the other hand, the values remain scattered at high water concentrations (>7 wt %), with the calculated results systematically overestimated relative the experimental data.

Obviously, the quality of fitting of the experimental data can be improved by taking into account the effect of still another parameters: the composition of the melt.

Equation (Zhang et al., 2007)

The authors of (Zhang et al., 2007) have further advanced efforts (Liu et al., 2005), but in contrast to the above two equations, they introduced one additional parameters into their equation: the agpaitic coefficient of the melt, which depends on its composition

$$C_w = \left(-0.231 + \frac{651.1}{T}\right)\sqrt{P}$$
$$+ \left(0.03424 - \frac{32.57}{T} + 0.02447 AI\right) P, \quad (3)$$

where C_w is the saturated water concentration (in wt %), T is the temperature (in K), P is the total pressure (in MPa), and $AI = (Na + K - Al)$, where Na, K, and Al

are the mole fractions of the respective components, and AI is the agpaitic coefficient.

Zhang et al., (2007) have derived this equation using a dataset of 93 selected experimental data points on felsic, intermediate, and mafic melts.

Comparison of the calculation results obtained with this model with experimental data from our dataset (Fig. 3) shows that the model better than the previous ones reproduces experimental values at low and intermediate water concentrations, but the calculated values at high water contents are systematically overestimated compared to the experimental ones.

Equation (Al'meev and Ariskin, 2007)

Another equation that accounts, in a simplified form, for the effect of melt composition on the solubility of pure H_2O in this melt is the equation in (Al'meev and Ariskin, 1996). The effect of melt composition on water solubility is accounted for by using the Si/O and Al/Si ratios

$$\ln C_{H_2O} = 4.39 + \frac{\left[38483\left(\frac{Si}{O}\right)^l - 14710\right]}{T}$$
$$+ 0.59 \ln P - 21.45\left(\frac{Si}{O}\right)^l + 3.89\left(\frac{Al}{Si}\right)^l, \quad (4)$$

where T is the temperature (in K), P is the pressure (in bar), melt parameters are in atomic units, and l is melt.
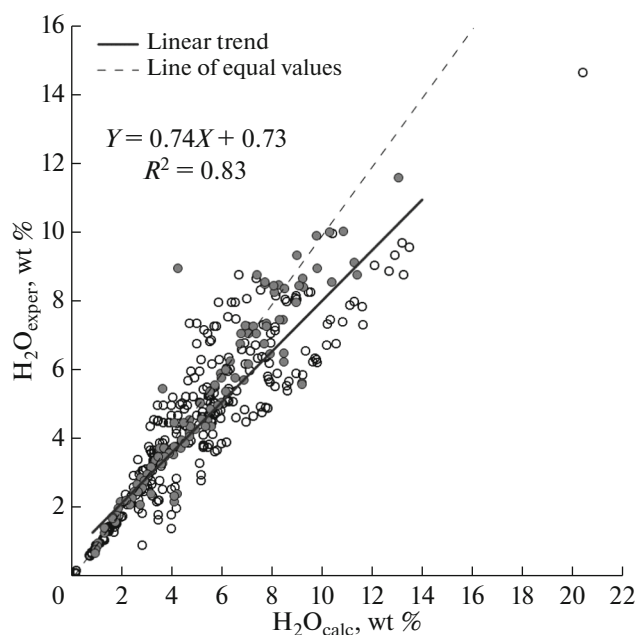
Fig. 4. Comparison of water solubility calculated by the model (Al'meev and Ariskin, 1996) with experimental data (data of 412 experiments in the dataset): solid circles are experimental data used by the authors to calibrate the equation, open symbols are other data from our dataset.

The ranges of intensive parameters of the dataset are as follows: temperature 800−1200°C, pressure is 200 bar to 9 kbar, dissolved water concentration is 0.5 to 12 wt %; the size of the dataset is 79 data points, and the compositions of the experimental systems cover a range from basalt to rhyolite.

Comparison of the calculated results and experimental data from our dataset is illustrated in Fig. 4. Comparison of Figs. 3 and 4 shows that the use of the Si/O and Al/Si ratios has not improved the reproducibility of the experimental data by the calculation results.

Equation (Moore et al., 1998)

The dependence of water solubility on melt composition is expressed in this equation through the mole fractions of Al_2O_3, FeO, and Na_2O normalized to the anhydrous silicate matrix (Moore et al., 1998):

$$2 \ln X_{H_2O}^{melt} = \frac{a}{T} + \sum b_i X_i \left(\frac{P}{T} \right) + c \ln f_{H_2O}^{fluid} + d, \quad (5)$$

where $X_{H_2O}^{melt}$ is the saturated mole fraction of water in melt, T is the temperature (in K), X_i is the oxide mole fraction in melt, P is the pressure (in bar), $f_{H_2O}^{fluid}$ is the water fugacity in the fluid (in bar), which is calculated by a modified Redlich−Kwong equation, a, b_i, and c are coefficients at respective variables, and d is a constant.

Inasmuch as water fugacity of pure water is close to the total pressure, we attempted to check how much the water concentrations calculated using its fugacity and total pressure are different. When the same coefficients were used, the maximal difference between the results calculated with these two approaches was no greater than 0.08 wt % H_2O (for 41 experiments by Moore et al., 1998). To simplify the Moore equation, we transformed it into

$$2 \ln X_{H_2O}^{melt} = \frac{a}{T} + \sum b_i X_i \left(\frac{P}{T} \right) + c \ln P + d. \quad (6)$$

The range of the intensive parameters of the dataset used in (Moore et al., 1998) is a temperature of 800−1200°C, pressure of 190 bar to 6 kbar, dissolved water content of 1.5 to 10 wt %; the size of the set is 41 experiments (with pure water fluid), samples of phonolite, andesite, and rhyolite composition.

Comparison of the results calculated by this model with experimental data from our dataset is illustrated in Fig. 5.

Analysis of Figs. 1−5 shows that each of the equations generally well reproduces experimental data that have been used by the authors to derive the coefficients of the respective equations, but experimental data from our greater dataset are best reproduced by the equation (Moore et al., 1998). This follows from the highest value of the coefficient of determination, the closeness of the slope of the regression line to unity, and the closeness of the constant term to zero.

However, this equation was derived based on a small set of experimental data (41 experiments), and hence, 25 years later we decided to recalibrate it on a greater amount of experimental data from our dataset.

In addition to models discussed above, the literature presents numerous other, more complicated models (e.g., Newman and Lowenstern, 2002; Papale et al., 2006 and references therein), but we decided to use the equation in (Moore et al., 1998) and consider more complicated models only if the relalibrated equation from (Moore et al., 1998) did not satisfy our requirements.

RECALIBRATED EQUATION (MOORE ET AL., 1998)

The recalibration procedure involved the selection of such values of the constants of Eq. (6) that optimally reproduced the experimental data. Equation (6) is linear with respect to the variables at the coefficients and the logarithm of water mole fraction. This seems to call for preferring multivariate linear regression in finding the coefficients and constant. This method is advantageous thanks to its good theoretical fundamentals and the ability to find the optimal values of the coefficients and constant with the assessment of their confidence (Vorob'ev, 2016).

However, the least-squares method attaches the greatest relative weight to data of the maximal value. When utilizing Eq. (6), we optimized the logarithms of water concentration expressed as a mole fraction. By definition, mole fractions are smaller than unity, and hence, the smaller the water concentration, greater the absolute values of the logarithms of this concentration. Thus, if the deviation of the logarithms are minimized, overestimated weights are acquired by low water contents. Analytical practice indicates that low concentrations are inevitably measured with greater inaccuracies, and hence, the risk is high that the derived dependence would predict disturbed concentrations. Indeed, Fig. 5 obviously demonstrates that the scatter of the data points is the greater, the higher water concentrations in melt. We have earlier faced this problem when deriving an equation for sulfur concentration in sulfide-saturated mafic melts (Koptev-Dvornikov et al., 2012), and this problem have been resolved by modifying the equation linear with respect to concentration logarithm to a form exponential with respect to the concentration itself and the direct optimization of the differences between the experimental and calculated concentrations (but not their logarithms). This transformation does not allow one to apply the apparatus of multivariate linear regression, which led us to apply the option SOLUTION SEARCH in MS Excel and the option SEARCH FOR SOLUTIONS OF NONLINEAR PROBLEMS BY MEANS OF GRG as the solution method.

Optimization of Exponential Equations

Equation (5) provides an expression for the saturated water mole fraction in melt

$$X_{H_2O}^{melt} = \exp^{\left(\frac{a}{T} + \sum b_i X_i \left(\frac{P}{T}\right) + cLnP + d\right)}, \tag{7}$$

where X_i are expressed as the mole fractions of the selected oxides in the single-cation form normalized to 100 wt % anhydrous basis. Note that we eliminated multiplier *2* when transforming Eq. (6).

Our experience in fitting experimental data by equations in form (7) demonstrates that the distributions of the excesses (differences between the calculated and experimental values of the optimized parameter) are close to normal (e.g., Koptev-Dvornikov et al., 2012; Koptev-Dvornikov and Bychkov, 2019). This also follows from the shapes of the histograms and the concordance criterion. The normality of the excess distributions makes it possible to assess the quality of the thermobarometers using the well-developed apparatus of statistics.

The quality of optimization is commonly assessed by the standard deviation (Herzberg and O'Hara, 2002 and many others). However, this approach is inaccurate because standard deviations characterize the mean deviations of an experimental value from the value calculated with a model but provides no infor-
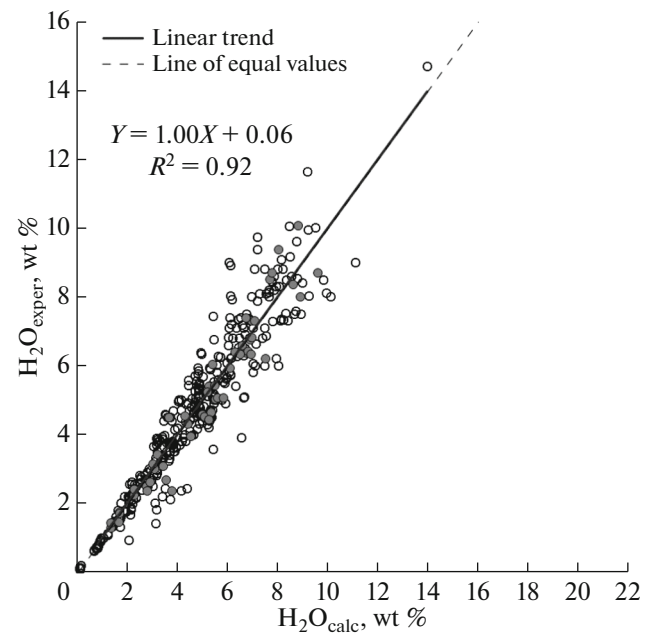

Fig. 5. Comparison of water solubility calculated by Eq. (6) with experimental data (data of 412 experiments in the dataset): solid circles are experimental data used in (Moore et al., 1998) to calibrate the equation, open symbols are other data from our dataset.

mation on the deviation of the value calculated with the model from the unknown real value.

A more accurate approach to assessing the approximation quality of experimental data is the use of confidence levels. An **advantage** of this approach is that confidence levels are targeted (in contrast to the standard deviation) not on assessing the quality of any single measurement but at determining (with a prespecified probability) the deviation limits of the calculated value from the real one. A useful property of confidence levels is that they can be determined for dependences (if the distribution is normal) and can be narrowed by increasing the number of measurements. Thanks to the large size of the dataset, the width of the confidence corridor is much lower than $\pm 2\sigma$ throughout the whole range of experimental values.

Based on our experience in optimizing equations that approximate experimental data, we decided to assess the quality of the prediction of this concentration by a corridor width at 95% confidence level.

Preparatorily to the recalibration of Eq. (7), we tested the optimality of the set of oxides proposed in (Moore et al., 1998). The best results were achieved when using mole fractions of FeO, CaO, and $NaO_{0.5}$ as the arguments. According to some literature data (Papale et al., 2006), water solubility may also notably depend on $KO_{0.5}$ concentration in the melt, but testing datasets that included concentrations of $KO_{0.5}$ or ($KO_{0.5} + NaO_{0.5}$) led us to conclude that the sums of
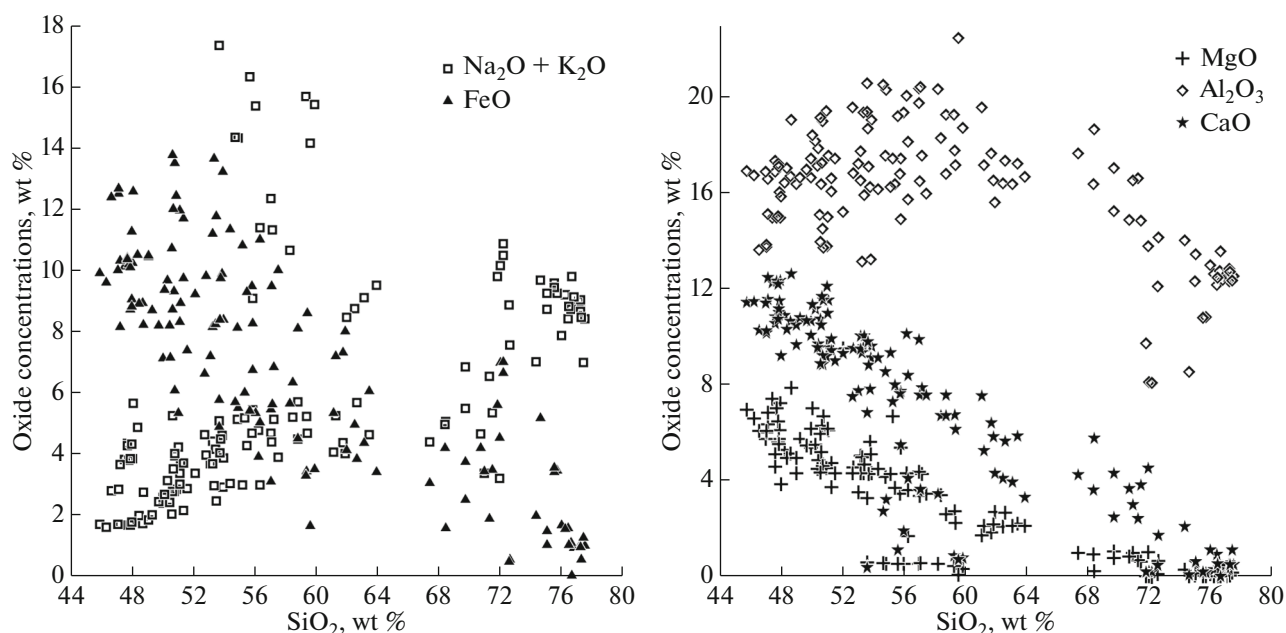
Fig. 6. Variations in the experimental melt compositions (394 experiments).

the squared excesses decreases therewith only very insignificantly (by 0.07%), in spite of the fact that $KO_{0.5}$ concentrations in our dataset broadly varied from 0 to 12.5 wt %, and the sums of ($K_2O + Na_2O$) ranged from 1.7 to 17.5 wt %.

In optimizing equations of form (7), we rejected data of experiments in which excesses were greater than 3σ, and this resulted in a reduction of the dataset to 394 experiments. Characteristics of the final dataset are presented in Table 1 and Fig. 6.

The polyhedron of 394 experimental melt compositions in coordinates of oxide concentrations for the final dataset is characterized by the following values (wt %): SiO_2 from 45.8 to 77.5, TiO_2 from 0 to 2.92, Al_2O_3 from 8 to 20.4, FeO^* from 0.1 to 13.74 (FeO^* is all Fe recalculated to FeO), MgO from 0 to 9.59, CaO from 0 to 12.6, Na_2O from 1.2 to 9.72, K_2O from 0 to 12.25, and P_2O_5 from 0 to 2.14. The dataset thus presents melt compositions ranging from basalt to rhyolite.

The ranges of the intensive parameters were as follows: temperature from 550 to 1300°C, pressure from 1 bar to 14.9 kbar, and oxygen fugacity $\log fO_2$ from −14.2 to −6.8.

Results of optimization with arguments of FeO, CaO, and $NaO_{0.5}$ mole fractions are displayed in Fig. 7a, and the coefficients of this equation are listed in Table 2.

Equations of form (7) are better to use in numerical simulations of magmatic evolution processes. At the same time, many researchers working with experimental or natural materials prefer to express water

concentrations in wt % and the arguments of the equations as concentrations (in wt %) of oxides in the melt normalized to anhydrous basis

$$C_{H_2O}^{melt} = \exp^{\left(\frac{a}{T} + \sum b_i C_i \left(\frac{P}{T}\right) + c \ln P + d\right)}, \quad (8)$$

where C_i is the wt % of oxides in the melts, $C_{H_2O}^{melt}$ is the saturated water concentration (in wt %), and other symbols as in Eq. (7).

Optimization results of Eq. (8) with arguments in the form of FeO, CaO, and $NaO_{0.5}$ concentrations (in wt %) are shown in Fig. 8, and the coefficients of this equation are listed in Table 3.

As follows from Fig. 7, the optimization of the exponential equation yields good results in both cases.

The experimental and calculation data displayed in Figs. 7a and 7b are obviously well consistent, as also follows from the closeness of the slope coefficients in the regression equation to unity and the absolute terms to zero, the closeness of the coefficients of determination, and the fairly small width of the confidence corridors. In Fig. 7a, the maximum width of the confidence corridor at high water concentrations is no greater than ±0.01 mole fraction (and is much smaller in the rest of the range). In Fig. 7b, the maximum width of the confidence corridor is ±0.2 wt %. The configurations of the histograms of the excesses in Fig. 7 indicate that the distributions are close to normal, and the estimated water solubility values are nonbiased. The calculated mean deviations of the calculated concentrations from experimental values (in mole fractions) are −0.000081, and those for the concentrations in wt % are 0.0042. The standard deviations are 0.017 and

Table 1. Characteristics of the dataset used to calibrate models for water solubility (394 experiments)

Number of experiments, N	T, °C	P, kbar	Composition	Method of water determination	References
9	1250	0.5−5	Tholeiite	FTIR, KFT	Shishkina et al., 2010
13	1000−1200	1−9	Basalt	Weight methods	Khitarov et al., 1968
1	1000	2	Basalt	Tritium autoradiography	Mironov et al.,1993
6	1200	0.2−0.7	Basalt	FTIR	Dixon et al., 1995
10	1045−1135	0.3−0.8	Basalt	FTIR	Metrich and Rutherford, 1998
21	1011−1090	1−2	Basalt	SIMS	Parman et al., 2011
1	901	14.9	Basalt	EPMA	Winther and Newton, 1991
28	910−1030	1−2	Basalt	EPMA	Erdman et al., 2015
3	980−1020	2	Basalt	EPMA	Feig et al., 2010
6	1200	0.5−5	Basalt	KFT	Berndt et al., 2002
6	1020−1100	1	High-Al basalt, basalt, andesite	FTIR	Sisson and Grove, 1993
3	1200	2	Fe-Basalt	FTIR	Botcharnikov et al., 2004
7	900−1000	1−2	Syenite	EPMA	Parat et al., 2010
1	1150	1.2	Basaltic andesite	EPMA	Muntener et al., 2001
11	1100	1−6.1	Basalt, andesite	Weight methods	Hamilton et al., 1964
10	1000−1200	1−5	Andesite	Weight methods	Kadik et al., 1986
8	1200−1250	0.5−3	Andesite, basalt	Manometry	Pineau et al., 1998
3	876−951	2−2.1	Andesite	EPMA, KFT	Martel et al., 1999
6	945−1025	3.9−4.3	Andesite, basalt	KFT	Pichavant et al., 2002
2	875−900	0.4−0.6	Phonolite	FTIR	Carrol and Blank., 1997
69	845−1200	0.5−3.95	Phonolite	Weight methods, KFT	Schmidt and Behrens, 2008
1	810	1	Rhyolite	SIMS	Mutch et al., 2016
3	650−800	1.5−1.6	Trachyte	EPMA	Scaillet and Macdonald, 2006
8	1000−1180	0.66−1.93	Rhyolite	EPMA	Moore et al., 1995
55	700−1300	0.1−3.5	Granite	Weight methods	Kadik et al., 1971
1	866	2.1	Dacite	EPMA	Scaillet and Evans, 1999
58	552−1200	0.001−0.3	Rhyolite, haplogranite	FTIR	Liu et al., 2005
2	800−900	1−2	Rhyolite	Weight methods	Shaw et al., 1963
6	850−1133	2	Rhyolite	EPMA	Baker and Rutherford, 1996
5	850	0.2−1.5	Rhyolite	FTIR	Silver et al., 1990
15	850−1200	0.22−1	Rhyolite	FTIR	Shigeru Yamashita, 1999
16	900−1100	1.8−3.1	Andesite, basaltic andesite, phonolite, trachyte, rhyolite, basalt	EPMA	Moore et al.,1998

FTIR is Fourrier transform IR spectroscopy;

KFT is Karl Fischer titration;

The weight methods involved determining the appearance of a fluid phase in equilibrium, mass losses on ignition, water absorption in Pregle tubes at incineration, and thermogravimetry;

SIMS is second-ion mass spectrometry

EPMA is electron probe microanalysis;

Manometry is measuring water pressure upon incineration in vacuum (at 1300°C).

The dataset is available on request at *gnuchevyakov@mail.ru; dmibychkov@gmail.com.*

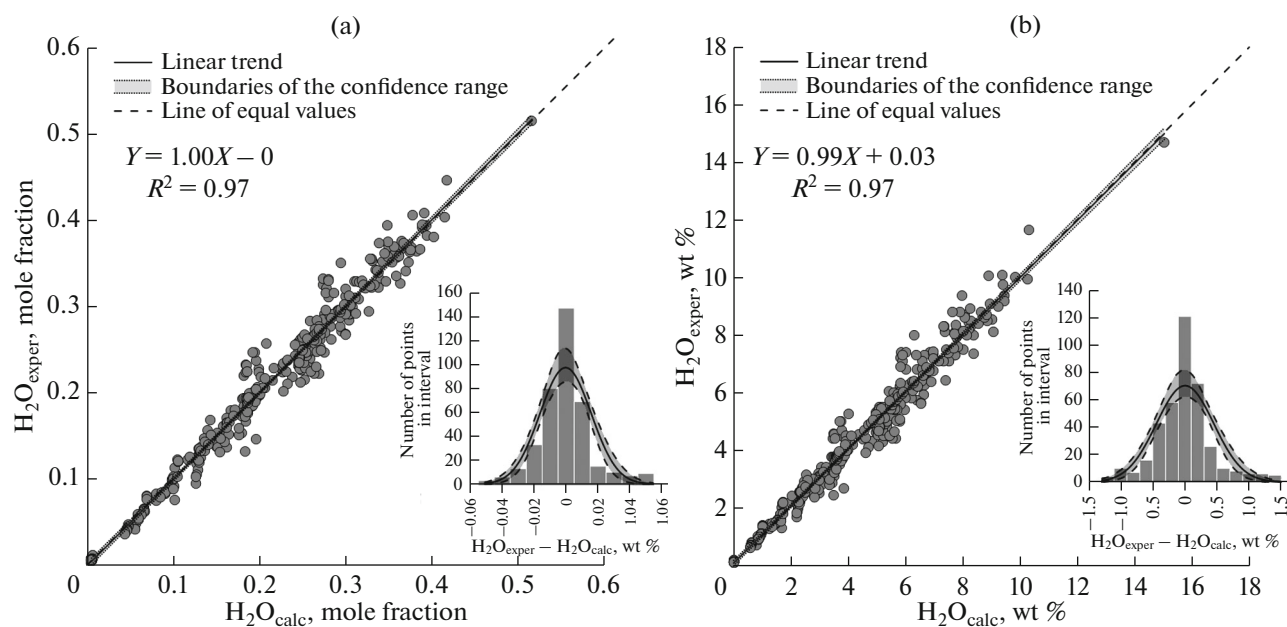The optimization results and the constant of Eq. (7) are presented in Table 2.

Fig. 7. (a) Optimization of Eq. (7); (b) optimization of exponential Eq. (8); dashed lines are the confidence intervals and 95% confidence. The dataset comprises information on 394 experiments.

0.45, and the deviation ranges of the calculated values from experimental ones are −0.051 to 0.059 in mole fractions and −1.29 to 1.66 in wt %.

Thus, optimization of equations for the calculation of water concentrations (in both mole fractions and wt %) show similar and fairly good results, in spite of that water concentrations in the experiments were analyzed by various techniques: FTIR, SIMS, tritium autoradiography, EPMA, Karl Fischer titration (KFT), and some other techniques (Table 1). These methods have been compared in (Devine et al., 1995; Shishkina et al., 2010; Schmidt and Behrens, 2008; Silver et al., 1990; and many others), and it has been proved that their results are highly consistent, with the greatest dispersion typical of the EPMA results, which are strongly dependent on the quality of the microprobe analysis. In view of this, the authors of the reviews suggest that this method should be selectively control by other techniques, which are more accurate but more time- and labor-consuming. Water concentrations in EPMA are calculated as the differences between analytical totals of 100 wt % and the total oxide concentrations determined by microprobe. The good consistency of results yielded by various analytical techniques for water concentrations is illustrated in Fig. 8 by the example of our dataset (412 experiments).

Table 2. Parameters of Eq. (7) obtained by optimizing data on a dataset of 394 experiments

a	b_{CaO}	b_{FeO}	$b_{NaO_{0.5}}$	c	d
440	−0.730	0.149	0.045	0.517	−5.55

As obviously seen in Fig. 8, the EPMA values show a broader dispersion, but nevertheless most of them does not disturb the general totality of our dataset.

AN EXAMPLE OF THE APPLICATION OF THE MODEL

The recently published paper (Crisp and Berry, 2022) stimulated us to demonstrate the usefulness of the model for water solubility in silicate melt. In this experimental study, conducted within broad ranges of temperature (800−1500°C), pressure (1 bar−40 kbar), and compositions of water-bearing melts, water concentrations were analyzed by EPMA. Using Eq. (8), we have calculated the saturated water concentration in melts for the experiments conducted under pressures no higher than 15 kbar (constraints on the pressure in our dataset) to make sure that the experimentally determined water concentration were no higher than the calculated values (in this set of 151 experiments). The results are presented in Fig. 9.

Figure 9 clearly demonstrates that the overwhelming majority of the data points plot within the field of melts unsaturated with water or close to the saturation line. Because the authors did not discuss water saturation in the melts, water concentrations in these experiments do not contradict the evaluations by Eq. (8). At the same time, doubt is provoked by the unrealistically high water concentrations in the products of 18 experiments conducted at 1 bar. The solution of Eq. (8) with respect to pressure leads to the conclusion that such dissolved water concentrations can be reached only under pressures of 3 to 7 kbar.
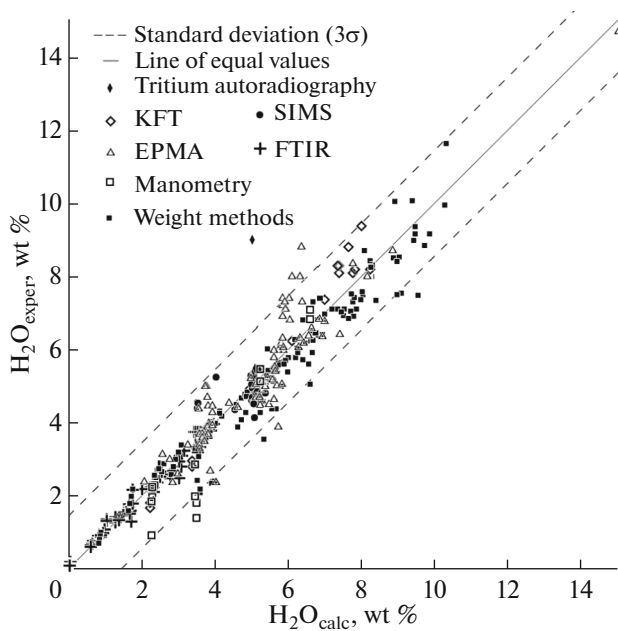
Fig. 8. Comparison of solubility calculated by Eq. (8) and coefficients in Table 3 with experimental data (412 experiments in the dataset).
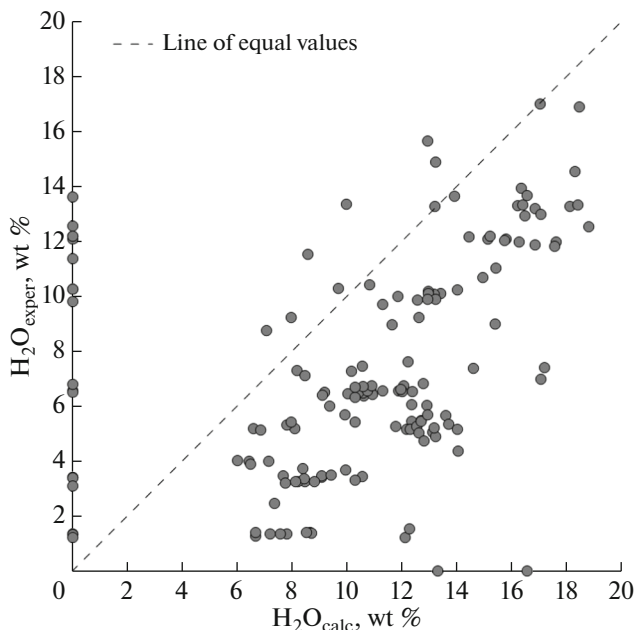

Fig. 9. Comparison of saturated water concentrations calculated by Eq. (8) and experimental data in (Crisp and Berry, 2022); 151 experiments in the dataset.

Table 3. Parameters of Eq. (8) obtained by optimizing data on a dataset of 394 experiments

a	b_{CaO}	b_{FeO}	b_{Na_2O}	c	d
447	−0.0094	0.0021	0.0050	0.628	−3.37

Inasmuch as the authors evaluated water concentrations by EPMA, it follows from the text of the paper that these evaluations have not been confirmed by analyses by other methods (in spite of the methodological recommendations), and hence, this approach puts in doubt the realism of the results pertaining to the water-bearing samples.

CONCLUSIONS

We have compiled a set of experimental data from the literature that comprises results of 394 quenching experiments characterizing water concentrations in melts within broad ranges of intensive parameters of silicate systems.

Analysis of the most popular types of models for water solubility in silicate melts indicate that the equation (Moore et al., 1998) best fits the experimental results.

The Moore equation recalibrated on the basis of an extended dataset enables predicting water concentrations in silicate melt within a compositional range from basalt to rhyolite, pressures up to 15 kbar, and temperatures of 550 to 1300°C with a maximum uncertainty of no greater than ±0.01 mole fraction or ±0.2 wt %.

CONFLICT OF INTEREST

The authors declare that they have no conflicts of interest.

REFERENCES

R. R. Al'meev and A. A. Ariskin, "Mineral−melt equilibria in a hydrous basaltic system: computer modeling," Geochem. Int. **34** (7), 563−573 (1996).

A. A. Ariskin and G. S. Barmina, *Modeling of Phase Equilibria during Crystallization of Basaltic Magmas* (Nauka/Interperiodika, Moscow, 2000) [in Russian].

A. A. Ariskin, G. S. Barmina, S. S. Meshalkin, G. S. Nikolaev, and R. R. Al'meev, "INFOREX−3.0: A database on experimental studies of phase equilibria in igneous rocks and synthetic systems: II. Data description and petrological applications," Comp. Geosci. **22** (10), 1073−1082 (1996).

A. A. Ariskin, S. S. Meshalkin, R. R. Almeev, G. S. Barmina, and G. S. Nikolaev, "INFOREX information retrieval system: analysis and processing of experimental data on phase equilibria in igneous rocks," Petrology **5** (1), 32−41 (1997).

N. S. Aryaeva, E. V. Koptev-Dvornikov, and D. A. Bychkov, "Liquidus thermobarometer for chromite−melt equilibrium modeling: development and verification," Moscow Univ. Geol. Bull. **71** (4), 337−346 (2016).

L. L. Baker and M. J. Rutherford, "The effect of dissolved water on the oxidation state of silicic melts," Geochim. Cosmochim. Acta. **60** (12), 2179−2187 (1996).

H. Behrens and N. Jantos, "The effect of anhydrous composition on water solubility in granitic melts," Am. Mineral. **86** (1−2), 14−20 (2001).

J. Berndt, C. Liebske, F. Holtz, M. Freise, M. Nowak, D. Ziegenbein, W. Hurkuck, and J. Koepke, "A combined rapid-quench and H_2-membrane setup for internally heated pressure vessels: Description and application for water solubility in basaltic melts," Am. Mineral. **87** (11−12), 1717−1726 (2002).

R. E. Botcharnikov, J. Koepke, F. Holtz, C. McCammon, and M. Wilke, "The effect of water activity on the oxidation and structural state of Fe in a ferro-basaltic melt," Geochim. Cosmochim. Acta **69** (21), 5071−5085 (2005).

M. R. Carroll and J. G. Blank, "The solubility of H_2O in phonolitic melts," Am. Mineral. **82** (5−6), 549−556 (1997).

J. D. Clemens, J. R. Holloway, and A. J. R. White, "Origin of an A-type granite: experimental constraints," Am. Mineral. **71** (3/4), 317−324 (1986).

L. J. Crisp and A. J. Berry, "A new model for zircon saturation in silicate melts," Contrib. Mineral. Petrol. **177** (7), 71 (2022).

J. D. Devine, J. E. Gardner, H. P. Brack, G. D. Layne, and M. J. Rutherford, "Comparison of microanalytical methods for estimating H_2O contents of silicic volcanic glasses," Am. Mineral. **80** (3−4), 319−328 (1995).

J. E. Dixon, E. M. Stolper, and J. R. Holloway, "An experimental study of water and carbon dioxide solubilities in mid-ocean ridge basaltic liquids. Part 1: Calibration and solubility models," J. Petrol. **36** (6), 1607−1631 (1995).

M. Erdmann, L. A. Fischer, L. France, C. Zhang, M. Godard, and J. Koepke, "Anatexis at the roof of an oceanic magma chamber at IODP Site 1256 (equatorial Pacific): an experimental study," Contrib. Mineral. Petrol. **169** (4), 1−28 (2015).

S. T. Feig, J. Koepke, and J. E. Snow, "Effect of oxygen fugacity and water on phase equilibria of a hydrous tholeiitic basalt," Contrib. Mineral. Petrol. **160** (4), 551−568 (2010).

D. L. Hamilton, C. W. Burnham, and E. F. Osborn, "The solubility of water and effects of oxygen fugacity and water content on crystallization in mafic magmas," J. Petrol. **5** (1), 21−39 (1964).

C. Herzberg and M. J. O'Hara, "Plume-associated ultramafic magmas of Phanerozoic age," J. Petrol. **43** (10), 1857−1883 (2002).

A. A. Kadik, E. B. Lebedev, and N. I. Khitarov, *Water in Magmatic Melts* (Nauka, Moscow, 1971).

A. A. Kadik, A. P. Maksimov, and B. V. Ivanov, *Physicochemical Conditions of Crystallization and Genesis of Andesites: Evidence from the Klyuchevskoy Group Volcanoes* (Nauka, Moscow, 1986).

N. I. Khitarov, A. A. Kadik, and E. B. Lebedev, "Water solubility in basaltic melts," Geokhimiya, No. 7, 763 (1986).

E. V. Koptev-Dvornikov and D. A. Bychkov, "Development of a liquidus thermobarometer to model the olivine−melt equilibrium," Moscow Univ. Geol. Bull. **74** (6), 592−605 (2019).

E. V. Koptev-Dvornikov, N. S. Aryaeva, and D. A. Bychkov, "Equation of thermobarometer for description of sulfide−silicate liquid immiscibility in basaltic systems," Petrology **20** (5), 495−495 (2012).

E. V. Koptev-Dvornikov, E. S. Romanova, and D. A. Bychkov, "Orthopyroxene thermobarometer−composition meter for the compositional range from magnesian basalts to dacites," *Tr. Vseross. Ezhegodn. Seminara Eksp. Mineral., Petrol., Geokhim.* (Moscow, 2020), pp. 74−77.

Y. Liu, Y. Zhang, and H. Behrens, "Solubility of H_2O in rhyolitic melts at low pressures and a new empirical model for mixed $H_2O−CO_2$ solubility in rhyolitic melts," J. Volcanol. Geotherm. Res. **143** (1−3), 219−235 (2005).

C. Martel, M. Pichavant, F. Holtz, B. Scaillet, J. L. Bourdier, and H. Traineau, "Effects of fO_2 and H_2O on andesite phase relations between 2 and 4 kbar," J. Geophys. Res.: Solid Earth. **104** (B12), 29453−29470 (1999).

N. Métrich and M. J. Rutherford, "Low-pressure crystallization paths of H_2O−saturated basaltic−hawaiitic melts from Mt Etna: Implications for open−system degassing of basaltic volcanoes," Geochim. Cosmochim. Acta. **62** (7), 1195−1205 (1998).

A. G. Mironov, M. B. Epelbaum, and A. S. Chekhmir, "Experimental determination of the relative solubility of water in granitic and basaltic melts at 900−1100°C and 2 kbar using tritium auoradiographic method," Geokhimiya, no. 4, 487−498 (1993).

G. Moore, K. Righter, and I. S. E. Carmichael, "The effect of dissolved water on the oxidation state of iron in natural silicate liquids," Contrib. Mineral. Petrol. **120** (2), 170−179 (1995).

G. Moore, T. Vennemann, and I. S.E. Carmichael, "An empirical model for the solubility of H_2O in magmas to 3 kilobars," Am. Mineral. **83** (1−2), 36−42 (1998).

O. Müntener, P. B. Kelemen, and T. L. Grove, "The role of H_2O during crystallization of primitive arc magmas under uppermost mantle conditions and genesis of igne-

ous pyroxenites: an experimental study," Contrib. Mineral. Petrol. **141** (6), 643−658 (2001).

E. J. F. Mutch, J. D. Blundy, B. C. Tattitch, F. J. Cooper, and R. A. Brooker, "An experimental study of amphibole stability in low-pressure granitic magmas and a revised Al-in-hornblende geobarometer," Contrib. Mineral. Petrol. **171** (10), 1−27 (2016).

S. Newman and J. B. Lowenstern, "VolatileCalc: a silicate melt−H_2O−CO_2 solution model written in Visual Basic for Excel," Comput. Geosci. **28** (5), 597−604 (2002).

P. Papale, R. Moretti, and D. Barbato, "The compositional dependence of the saturation surface of H_2O + CO_2 fluids in silicate melts," Chem. Geol. **229** (1−3), 78−95 (2006).

F. Parat, F. Holtz, M. René, and R. Al'meev, "Experimental constraints on ultrapotassic magmatism from the Bohemian Massif (durbachite series, Czech Republic)," Contrib. Mineral. Petrol. **159** (3), 331−347 (2010).

S. W. Parman, T. L. Grove, K. A. Kelley, and T. Plank, "Along-arc variations in the pre-eruptive H_2O contents of Mariana arc magmas inferred from fractionation paths," J. Petrol. **52** (2), 257−278 (2011).

M. Pichavant, C. Martel, J. L. Bourdier, and B. Scaillet, "Physical conditions, structure, and dynamics of a zoned magma chamber: Mount Pelée (Martinique, Lesser Antilles Arc)," J. Geophys. Res.: Solid Earth. **107** (B5), ECV−1 (2002).

F. Pineau, S. Shilobreeva, A. Kadik, and M. Javoy, "Water solubility and D/H fractionation in the system basaltic andesite−H_2O at 1250 C and between 0.5 and 3 kbars," Chem. Geol. **147** (1−2), 173−184 (1998).

E. S. Romanova, E. V. Koptev-Dvornikov, and D. A. Bychkov, "Pigeonite liquidus termobarometer for the compositional range of melts from magnesian basalts to dacites," *Tr. Vseross. Ezhegodn. Seminara Eksp. Mineral., Petrol., Geokhim.* (Moscow, 2020), pp. 90−93 [in Russian].

B. Scaillet and B. W. Evans, "The 15 June 1991 eruption of Mount Pinatubo. I. Phase equilibria and pre-eruption P−T−fO_2−fH_2O conditions of the dacite magma," J. Petrol. **40** (3), 381−411 (1999).

B. Scaillet and R. Macdonald, "Experimental constraints on pre-eruption conditions of pantelleritic magmas: evidence from the Eburru complex, Kenya Rift," Lithos. **91** (1−4), 95−108 (2006).

B. C. Schmidt and H. Behrens, "Water solubility in phonolite melts: Influence of melt composition and temperature," Chem. Geol. **256** (3−4), 259−268 (2008).

H. R. Shaw, "Obsidian−H_2O viscosities at 1000 and 2000 bars in the temperature range 700° to 900°C," J. Geophys. Res. **68** (23), 6337−6343 (1963).

T. A. Shishkina, R. E. Botcharnikov, F. Holtz, R. R. Almeev, and M. V. Portnyagin, "Solubility of H_2O-and CO_2-bearing fluids in tholeiitic basalts at pressures up to 500 MPa," Chem. Geol. **277** (1−2), 115−125 (2010).

L. A. Silver, P. D. Ihinger, and E. Stolper, "The influence of bulk composition on the speciation of water in silicate glasses," Contrib. Mineral. Petrol. **104** (2), 142−162 (1990).

T. W. Sisson and T. L. Grove, "Temperatures and H_2O contents of low-MgO high-alumina basalts," Contrib. Mineral. Petrol. **113** (2), 167−184 (1993).

S. A. Vorobev, *Informatics. Mathematical Processing of Geological-Geochemical Data, A Textbook* (Novyi format, Barnaul, 2016) [in Russian].

K. T. Winther and R. C. Newton, "Experimental melting of hydrous low-K tholeiite: evidence on the origin of Archaean cratons," Bull. Geol. Soc. Den. **39**, 213−228 (1991).

S. Yamashita, "Experimental study of the effect of temperature on water solubility in natural rhyolite melt to 100 MPa," J. Petrol. **40** (10), 1497−1507 (1999).

Y. Zhang, Z. Xu, M. Zhu, and H. Wang, "Silicate melt properties and volcanic eruptions," Rev. Geophys. **45** (4) (2007).

Translated by E. Kurdyukov